SIMULACIÓN Y APLICACIONES RECIENTES PARA CIENCIA Y TECNOLOGÍA
Y. González, E. Dávila, V. Duarte, M. Candal, O.Pelliccioni, J. Darias, M. Cerrolaza (Editores)

A MIMETIC WAVE EQUATION DISCRETIZATION WITH ABSORBING BOUNDARY CONDITION: FORMULATION AND APPLICATION

Freysimar Solano-Feo
Juan M. Guevara-Jordan
Otilio Rojas
Carlos L. González-Ramírez.
freysimar15@gmail.com
jmguevarajordan@gmail.com
rojasotilio@gmail.com
carlosl.gonzalez.ucv@gmail.com
Facultad de Ciencias, Universidad Central de Venezuela, Caracas, Venezuela.
Beatriz Otero
botero@ac.upc.edu
Dpto. de Arquitectura d'Computadors, Universitat Politécnica de Catalunya, Campus Nord, Barcelona, Spain.

Abstract. *The cornerstone of mimetic finite differentiation (FD) is that discrete gradients and divergences, in combination with a novel boundary flux operator satisfies an approximation to the Gauss–Divergence theorem. In this paper, we propose a spatially staggered second-order discretization of the acoustic wave equation that fully exploits all these mimetic operators on the implementation of free surface and absorbing boundary conditions. Explicit time integration is carried out by using the standard three-level central FD stencil. Applications of this new method to simple 2-D seismic scenarios are also presented and discussed.*

Key words: Acoustic wave, absorbing, mimetic finite differences, staggered grids, Reflection.

1 INTRODUCTION

Modeling acoustic and elastic propagation in realistic seismic scenarios demands effective implementations of free surfaces (FS) and absorbing boundary conditions (ABC). Reynolds in [1] constructs a family of splitting operators by considering acoustic and elastic domains. The application of Reynolds's ABC proceeds by compositions of these first order differential operators that progressively increase their effectiveness and at the same time increases complexity of its implementation.

Finite difference schemes (FD) on staggered grids have been widely used in the modeling of seismic waves because of its easy implementation. However, these methods are

voluminous, have a very high computational cost and they do not preserve fundamental properties of differential calculus, including a sloppy treatment of the boundary conditions.

A big enhancement, are the mimetic methods which came from the extensive works of Samarsky [2]. These has evolved into two modern methods on SG. The first one is based on two discrete support operators, the Divergence D and the Gradient G, both providing second-order accuracy at interior grid points, but reduced to first order at domain boundaries. This method has been extensively applied to difussion, electromagnetic, and viscoelastic problems even on non-uniform meshes [3, 4]. The other method for conservative operators, D and G exhibits second, fourth, and sixth order accuracy along all grid locations including boundaries. This method was proposed by Castillo and collaborators in [5] and later reformulated in [6] by the authors. For a rigorous numerical treatment of Neumann and Robin boundary conditions, Castillo and Yasuda [7] introduces an operator B to approximate boundary fluxes of a given vector field. These new operators D, G and B, are referred as mimetic because in combination with the numerical solution to a boundary value problem, they satisfies a particular discrete version of the celebrated Green-Stoke-Gauss Theorem.

Applications of these mimetic operators D and G have been widely studied by Rojas and collaborators in the modeling of in-plane ruptures over cartesian staggered grid (SG) [8, 9, 10].

In this article, we propose a fully mimetic method for acoustic wave propagation on 1-D and 2-D rectangular SG. The combined operator DG approximates the Laplacian at interior grid nodes and BG allows the boundary (free surface and absorbing) condition enforcement at grid edges. However, operator BG also adds a significant contribution to the Laplacian at grid points neighbors to boundary lines. Consequences on the stability and consistency for this method are also studied. Formulations and convergence analysis of these mimetic schemes are given in the first four sections. The current implementation applies first-order Reynold's ABC operators at artificial boundaries and satisfactory results have been observed in two interesting 2-D tests which will be presented in section 5. The first test consists in a homogeneous model and the second one in a three layered heterogeneous model with horizontal stratification. Both tests are presented with a combination of two different kinds of boundary conditions. Conclusions and some guidelines for future works are given in section 6.

2 THE ACOUSTIC WAVE EQUATION

In this work, we apply the mimetic discretization procedure to the second order formulation of the acoustic wave equation. The physical interpretation of the unknown solution would vary from 1-D to 2-D spatial domains, as we explain below.

2.1 1-D Formulation

The displacement u of particles in a 1-D acoustic medium satisfies the following equation

$$\frac{\partial^2 u}{\partial t^2} - c^2 \frac{\partial^2 u}{\partial x^2} = f(x,t), \tag{1}$$

where c represents the wave speed and $f(x,t)$ is the source term. In the following sections, we assume that $x \in [0,a]$, $t \geq 0$, and the initial condition is $u(x,0) = \frac{\partial u}{\partial t} = 0$. We also consider boundary conditions of the form

$$\frac{\partial u}{\partial x}(0,t) = f_1(t), \tag{2}$$

$$\left[\frac{\partial u}{\partial t} + c\frac{\partial u}{\partial x}\right](a,t) = f_2(t). \tag{3}$$

In the case when $f_1(t) = f_2(t) = 0$, Eq. (2) represents a Neumann condition (FS), while Eq. (3) models outgoing waves through $x = a$ that Reynolds [1] defines as a first order ABC operator.

2.2 2-D Formulation

In this section, we are going to extend the wave propagation model described above to a 2-D rectangular domain given by the following equation

$$\frac{\partial^2 u}{\partial t^2} - c^2\nabla^2 u = f(x,z,t), \qquad (x,z) \in [0,a] \times [0,b], \tag{4}$$

where u represents the acoustic pressure of the wave.

In the above equation, ∇^2 represents the Laplacian operator, and similarly to the 1-D case c and f denote the wave speed and the seismic source, respectively. In this case, we associate the rectangle edges $x = 0$, $x = a$ and $z = 0$ with artificial absorbing boundaries conditions, and set up $z = b$ as the free surface. Thus,

$$\left(\frac{\partial u}{\partial t} - c\frac{\partial u}{\partial x}\right)(0,z,t) = 0, \tag{5}$$

$$\left(\frac{\partial u}{\partial t} + c\frac{\partial u}{\partial z}\right)(a,z,t) = 0, \tag{6}$$

$$\left(\frac{\partial u}{\partial t} - c\frac{\partial u}{\partial z}\right)(x,b,t) = 0, \tag{7}$$

$$u(x,0,t) = 0. \tag{8}$$

It is appropriate to note that this time the FS condition (8) is a Dirichlet type boundary condition.

3 MIMETIC METHOD

The mimetic discretization of a Boundary Value Problem (BVP) proceeds in the spatial domain by substituting the continuous differential operators gradient (∇), divergence ($\nabla.$) and the normal derivative ($\frac{\partial}{\partial \bar{n}}$) at boundaries by the discrete versions G, D, and BG proposed in [6] and [7]. These mimetic operators satisfy the following approximation to the Green's Identity

$$\langle Dv, u\rangle_Q + \langle v, Gu\rangle_P = \langle Bv, u\rangle_I, \tag{9}$$

with the inner product $\langle \cdot, \cdot \rangle_A$ defined by

$$\langle x, y\rangle_A = y^t A x, \qquad (x, y \in \mathbb{R}^n),$$

where A is positive definite matrix. On the other hand, the discretization of directional derivative at the border satisfies the following expression:

$$B = QD + G^t P, \tag{10}$$

where I, Q and P are weight diagonal matrices that agree with the coefficients of mid-point quadrature and $\frac{3}{8}$ Newton-Cotes quadrature.

The matrix representations of operators D, G and B depends on the discretization of scalar and vector fields u and v respectively. In the 1-D case, Castillo and collaborators discretized the domain $[0, a]$ by using uniform cells $[x_i, x_{i+1}]$ with nodes $x_i = ih$ for $i = 0, \ldots, (n-1)$ and grid step $h = \frac{a}{n}$. This grid becomes staggered by including the cell centers $x_{i+\frac{1}{2}} = \frac{x_i + x_{i+1}}{2}$. Discrete values of the function u are considered at cell centers $x_{i+\frac{1}{2}}$ in addition to the boundary values at x_0 and x_n. Evaluations of the function v are placed only at grid nodes. For simplicity, Fig. 1(a) just depicts the grid distribution of discrete u values which are collected in the vector $\vec{u}$. Similarly, a vector $\vec{v}$ allows storing evaluations of the field v.

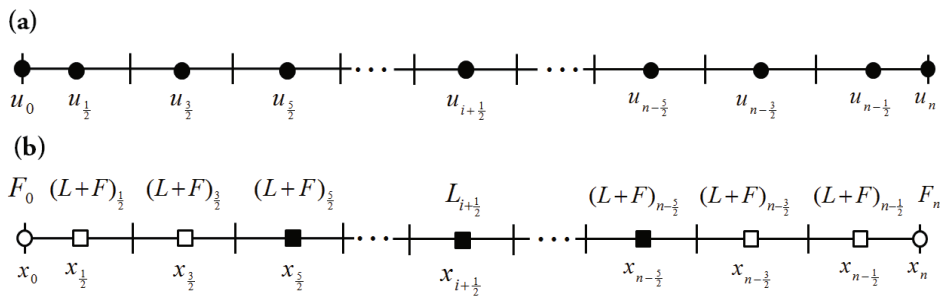

Figure 1: 1-D mimetic differentiation grid for the function u using mimetic operator: B, G and D. $L = DG$ represent the laplacian operator discretization and $F = BG$ the flux operation discretization in the border of grid.

Numerical differentiation of u is computed by $G\vec{u}$ which renders $n+1$ approximations to $\frac{du}{dx}$, for each grid node. In the same way, $D\vec{v}$ yields to approximations of $\frac{dv}{dx}$ at the n cell centers. Second order accurate mimetic gradient and divergence operators are given by

$$G = \frac{1}{h}\begin{pmatrix} -\frac{8}{3} & 3 & -\frac{1}{3} & 0 & \ldots & 0 \\ 0 & -1 & 1 & 0 & \ldots & 0 \\ \vdots & & \ddots & \ddots & & \vdots \\ 0 & \ldots & 0 & -1 & 1 & 0 \\ 0 & \ldots & 0 & \frac{1}{3} & -3 & \frac{8}{3} \end{pmatrix}, \quad D = \frac{1}{h}\begin{pmatrix} 0 & 0 & 0 & 0 & \ldots & 0 \\ -1 & 1 & 0 & 0 & \ldots & 0 \\ \vdots & & \ddots & \ddots & & \vdots \\ 0 & \ldots & 0 & 0 & -1 & 1 \\ 0 & 0 & 0 & 0 & \ldots & 0 \end{pmatrix}.$$

The first and last row of operator G corresponds to lateral discretization of boundary nodes, which are obtained by Taylor expansions. The non-zero rows of operator D are given by the classical finite difference step-forward formula for interior mesh nodes and

this present a second order accuracy. Authors in [5] and [6] established these differential operators with higher order. On the other hand, the mimetic operator D exhibits zeros along its first and last rows to allow a convenient accommodations of Neumann or Robin boundary conditions, as we show in next section.

According to these definitions and the above expressions for D and G, the flux operator B follows from Eq. (10)

$$B = \begin{pmatrix} -1 & 0 & 0 & & \dots & & 0 \\ \frac{1}{8} & -\frac{1}{8} & 0 & & \dots & & 0 \\ -\frac{1}{8} & \frac{1}{8} & 0 & & \dots & & 0 \\ 0 & 0 & 0 & & \dots & & 0 \\ \vdots & \vdots & \vdots & \ddots & \vdots & \vdots & \vdots \\ 0 & & \dots & & 0 & -\frac{1}{8} & \frac{1}{8} \\ 0 & & \dots & & 0 & \frac{1}{8} & -\frac{1}{8} \\ 0 & & \dots & & 0 & 0 & 1 \end{pmatrix}.$$

First and last rows in B represent the outward normal vector at grid boundaries and the same rows in the composed operator BG (denoted as F in Fig. 1(b)) allows to approximate $\frac{\partial u}{\partial \vec{n}}$ at both boundaries. The non zero interior rows of B add an important contribution to the Laplacian approximation $L = GD$ at the two nearest cell centers to each grid boundary (denoted as $F + L$ in Fig. 1(b)). The remaining zero rows in B do not affect laplacian calculations at interior cell centers (as also shown by Fig. 1(b)).

4 DISCRETIZATION OF ACOUSTIC WAVE EQUATION

4.1 1-D Case

Here we present, based upon matricial structures of the mimetic operators the discretization for each node of the mesh. Let u_i^k denotes the displacement at time $t = k\Delta t$ and at spacial location $x = ih$, with $i = 0, \dots, n$, where Δt denotes the time step size and h is the step-size between nodes in the x direction.

We apply standard central differentiation for the time

$$u_{tt}(ih, k\Delta t) \approx \frac{u_i^{k+1} - 2u_i^k + u_i^{k-1}}{\Delta t^2},$$

and the spacial approximation for the cell center $x_{i+\frac{1}{2}}$ are given by

$$\frac{u_{i+\frac{1}{2}}^{k+1} - 2u_{i+\frac{1}{2}}^k + u_{i+\frac{1}{2}}^{k-1}}{\Delta t^2} = \left(\frac{c}{h}\right)^2 \left[u_{i+\frac{3}{2}}^k - 2u_{i+\frac{1}{2}}^k + u_{i-\frac{1}{2}}^k\right], \tag{11}$$

where the last term on the right hand side corresponds to the standard SG discretization of Laplacian $L_{i+\frac{1}{2}}$. Now, at the cells center $x_{\frac{1}{2}}$ and $x_{\frac{3}{2}}$ the spacial approximation is replaced

by

$$(L+F)_{\frac{1}{2}} = \left(\frac{8c^2}{3h^2} - \frac{c}{3h}\right)u_0^k + \left(\frac{c}{2h} - \frac{4c^2}{h^2}\right)u_{\frac{1}{2}}^k + \left(\frac{4c^2}{3h^2} - \frac{c}{6h}\right)u_{\frac{3}{2}}^k, \tag{12}$$

$$(L+F)_{\frac{3}{2}} = \left(\frac{c}{3h}\right)u_0^k + \left(\frac{c^2}{h^2} - \frac{c}{2h}\right)u_{\frac{1}{2}}^k + \left(\frac{c}{6h} - \frac{2c^2}{h^2}\right)u_{\frac{3}{2}}^k + \left(\frac{c^2}{h^2}\right)u_{\frac{5}{2}}^k. \tag{13}$$

The cases $x_{n-\frac{1}{2}}$ and $x_{n-\frac{3}{2}}$ are analogous and we omit them. The spacial discretization at boundary points is given by the contribution of both the flux and gradient operators

$$B_0 = -\frac{8}{3h}u_0^k + \frac{3}{h}u_{\frac{1}{2}}^k - \frac{1}{3h}u_{\frac{3}{2}}^k. \tag{14}$$

For the discretization at border node x_n, we have used a step-forward difference for the time variable, while for the space variable we have used an approximation given by (14) except for the change of signs To analyze the consistency we use Taylor expansions. It is easy to see that the error at boundary points x_0, x_n and the cell center $x_{i+\frac{1}{2}}$ is $O(h^2)$. Here we present the truncation errors for the cases of interest:

$$(L+F)_{\frac{1}{2}} - c^2\frac{\partial^2 u}{\partial x^2}(x_{\frac{1}{2}}) = \frac{1}{8}h\frac{\partial^2 u}{\partial x^2} = O(h), \qquad (L+F)_{\frac{3}{2}} - c^2\frac{\partial^2 u}{\partial x^2}(x_{\frac{3}{2}}) = -\frac{1}{8}h\frac{\partial^2 u}{\partial x^2} = O(h)$$

The study of errors for the cases $x_{n-\frac{1}{2}}$ and $x_{n-\frac{3}{2}}$ are analogous, except for change of signs. The results obtained show that the boundary condition equations, and the equations for interiors nodes exhibit quadratic truncation error, while the equations for nodes close to the border edges present linear truncation errors and are consistent with the wave equation and its boundary conditions. A stability analysis showed that the new scheme is stable for a courant value of $\frac{c\Delta t}{h} < \frac{\sqrt{3}}{2}$ whose condition is better than standard finite difference scheme on staggered grids.

4.2 2-D Case

The elaboration of the mimetic mesh in various variables are obtained by the usual cartesian product or the tensor product of one-dimensional grid in each coordinate direction and eliminating the points corresponding to the corners. In Fig. 2 is presented the mimetic grid for the bidimensional case. The gradient operator is now a vector with two components G_x and G_z, which are evaluated at each midpoint of the four edges of every block on the grid. The solution u and the G operator are evaluated in the borders. The divergence operator D is evaluated only in the interior nodes or in the centers blocks. In terms of the matricial structures showed above we have discretized our problem of contour in the following form: we consider a staggered mesh that represents a uniform partition $N_x \times N_z$ of the domain D with N_x the number of nodes in the partition corresponding to the x axis and N_z the number of nodes in the partition corresponding to the z axis, h is the space between mesh nodes and Δt represents the time step.

We consider the rectangular domain $D := [0, a] \times [0, b]$ and denote by u_{ij}^k the numerical approximation of $u(x_i, z_j, t_k)$, where $x_i = ih$, with $i \in \{0, \ldots, N_x\}$, $z_j = jh$, with $j \in \{0, \ldots, N_z\}$ and $t_k = k\Delta t$, with $k \in \{0, \ldots, T_f\}$, where T_f is the final simulation time.

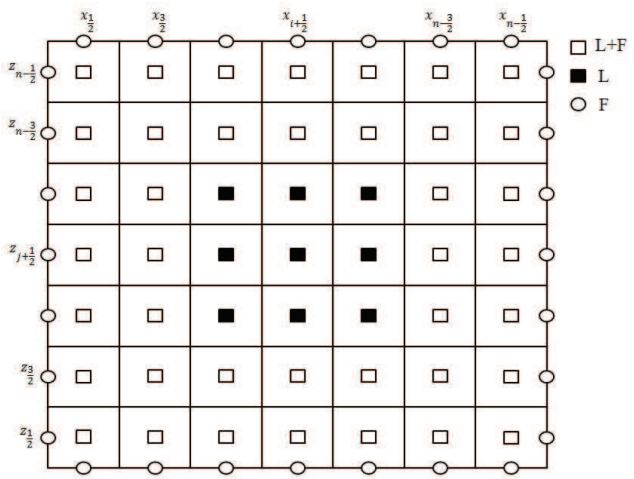

Figure 2: 2-D mimetic differentiation grid. The approximation for the border nodes are represented by $F = BG$ (flux operator), in the interior nodes nearby to the borders are using $L + F$ and the interior nodes are using only the laplacian operator ($L = DG$).

In the bidimensional case the discretizations are generalizations of the one-dimensional case, thus we only show the discretization for some mesh nodes. The boundary nodes are analogous to the Eq.(14). By symmetry and except by a sign change, we will only show some stencils for the mimetic mesh of Fig. 2:

- Node $\circ$: $u(x_i, z_j)$ for $i = 0$ and $j \in \{\frac{1}{2}, \ldots, N_y - \frac{1}{2}\}$,

$$u_{ij}^{k+1} = u_{ij}^{k} + \left(\frac{c\Delta t}{h}\right)\left[-\frac{8}{3}u_{ij}^{k} + 3u_{i+\frac{1}{2}j}^{k} - \frac{1}{3}u_{i+\frac{3}{2}j}^{k}\right]. \tag{15}$$

- Node $\square$: $u(x_i, z_j)$ for $i \in \{\frac{1}{2}, N_x - \frac{1}{2}\}$ and $j \in \{\frac{1}{2}, N_y - \frac{1}{2}\}$,

$$\begin{aligned} u_{ij}^{k+1} &= 2u_{ij}^{k} - u_{ij}^{k-1} + \Delta t^2\left[\left(\frac{8c^2}{3h^2} - \frac{c}{3h}\right)u_{i-\frac{1}{2},j}^{k} + \left(\frac{c}{2h} - \frac{6c^2}{h^2}\right)u_{i,j}^{k}\right. \\ &\left. + \left(\frac{4c^2}{3h^2} - \frac{c}{6h}\right)u_{i\pm1,j}^{k} + \left(\frac{c^2}{h^2}\right)u_{i,j+1}^{k} + \left(\frac{c^2}{h^2}\right)u_{i,j-\frac{1}{2}}^{k}\right]. \end{aligned} \tag{16}$$

- Node $\square$: $u(x_i, z_j)$ for $i \in \{\frac{3}{2}, N_x - \frac{3}{2}\}$ and $j \in \{\frac{5}{2}, \ldots, N_y - \frac{5}{2}\}$,

$$\begin{aligned} u_{ij}^{k+1} &= 2u_{ij}^{k} - u_{ij}^{k-1} + \Delta t^2\left[\left(\frac{c^2}{h^2} - \frac{c}{2h}\right)u_{i\mp1,j}^{k} + \left(\frac{c}{6h} - \frac{4c^2}{h^2}\right)u_{i,j}^{k}\right. \\ &\left. + \left(\frac{c}{3h}\right)u_{i-\frac{3}{2},j}^{k} + \left(\frac{c^2}{h^2}\right)u_{i\pm1,j}^{k} + \left(\frac{c^2}{h^2}\right)u_{i,j-1}^{k} + \left(\frac{c^2}{h^2}\right)u_{i,j+1}^{k}\right]. \end{aligned} \tag{17}$$

- Node $\bullet$: $u(x_i, z_j)$ for $i \in \{\frac{5}{2}, \ldots, N_x - \frac{5}{2}\}$ and $j \in \{\frac{5}{2}, \ldots, N_y - \frac{5}{2}\}$,

$$u_{ij}^{k+1} = 2u_{ij}^{k} - u_{ij}^{k-1} + \left(\frac{c\Delta t}{h}\right)^2\left[u_{i-1,j}^{k} + u_{i+1,j}^{k} - 4u_{ij}^{k} + u_{i,j-1}^{k} + u_{i,j+1}^{k}\right]. \tag{18}$$

5 SIMULATION IN A 2-D LAYERED MODEL

In this section we present two numeric tests of seismic traces obtained by applying a point shallowed source located over two media earthbounds: an homogeneous squared media and a heterogeneous rectangular three layered media with horizontal stratification. In both tests we have used the new mimetic numerical scheme with different kinds of boundary conditions.

5.1 Homogeneous Model

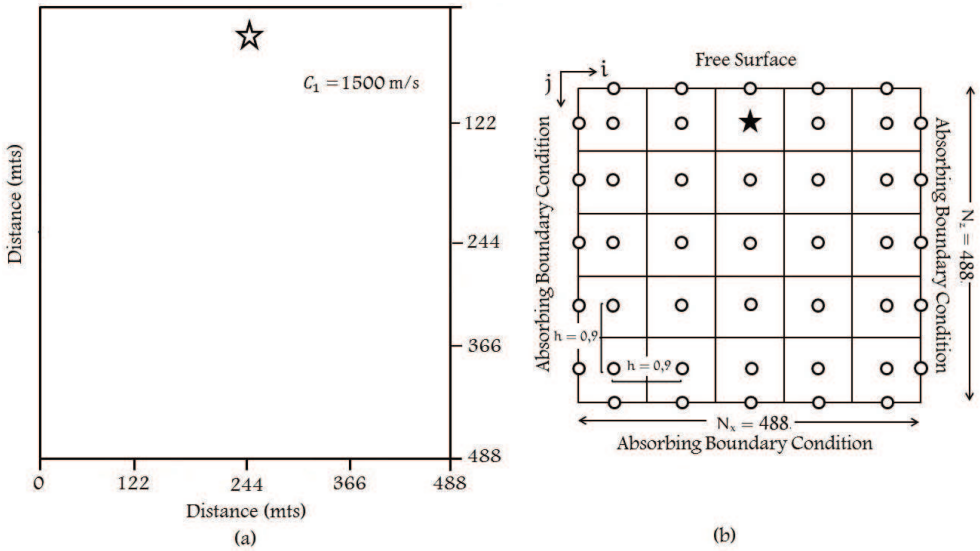

Figure 3: (a) Velocity model and geometry. (b) Computational region with a staggered grid.

This numerical test is based upon the research made it by Reynolds in [1] for the homogeneous case with a Ricker source centered at 37m from the surface. This piece of land is a squared extension of 488m long, with a constant speed of 1500 m/s. We build over this terrain a uniform distributed staggered grid with 500×500 nodes, separated by h=0.9m as in Fig. 3(b). The wave is received by one hundred receptors which are located at the top of the surface, each of them with a separation of 5m from its neighbors. Fig. 3(a) shows up the model of terrain we are modeling, while Fig. 3(b) shows the computational domain used in our discretization.

The study of seismic traces is based on two boundary problems. One of them consists in a combination of two kinds of boundary conditions: a free boundary condition at the top border which are well-known as Dirichlet-type boundary condition and it is given by Eq. (8). The other one is a first order absorbing boundary condition which is defined at the side and bottom borders of the domain and are given by equation (5)-(7). The seismic traces of this problem can be observed in Fig. 4 where one can appreciate only one wave corresponding to the direct wave obtained from the source term.

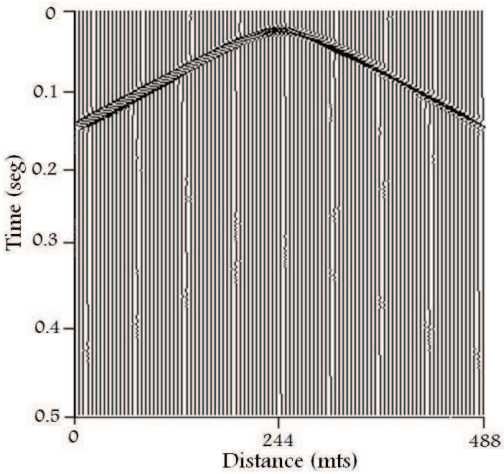

Figure 4: Seismic traces for absorbing conditions.

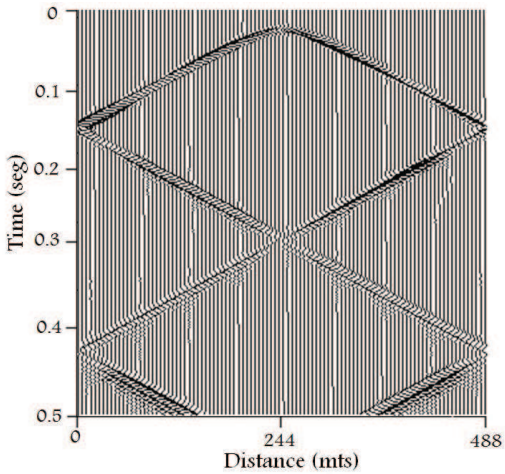

Figure 5: Seismic traces for Dirichlet conditions.

The other problem is conformed only by Dirichet-type boundary conditions at every border of the domain, and these results are shown in Fig. 5 where it can be seen that between the arrival times 0.1s and 0.2s the strong reflections of the direct wave because of the collision with lateral borders of the discrete domain.

5.2 Heterogeneous Model

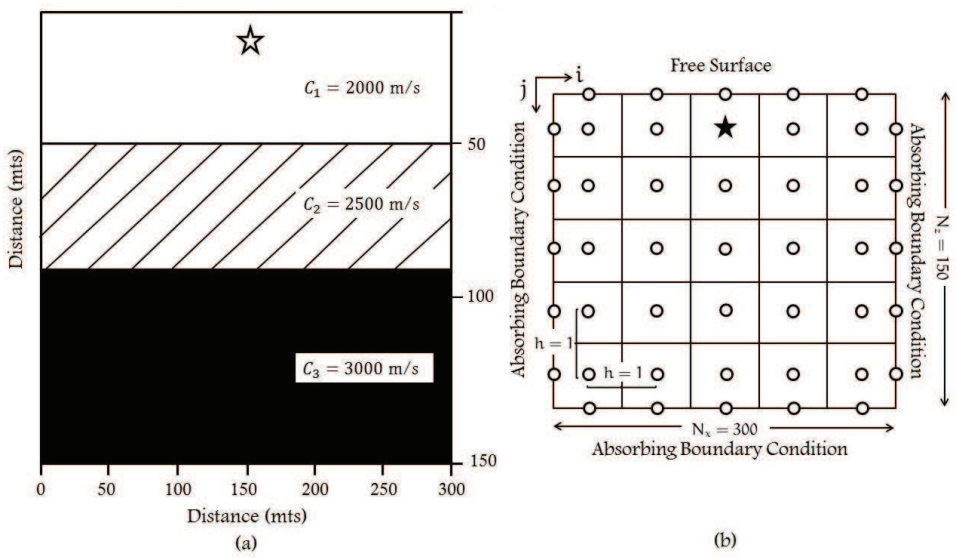

Figure 6: (a) Velocity model and geometry. (b) Computational region with a staggered grid.

This problem is based on the model [11] and its structure is show in Fig. 6(a). This earthbound model is represented by a rectangular section which has an extension of 300m

long (horizontal direction) and 150m deep (vertical direction). This terrain is divided in three layers with horizontal stratification and their speeds are show in Fig. 6(a). As is specified in Fig. 6(a), this region is covered by a uniform distributed staggered grid with 300×150 nodes and the spaced between blocks is 1m length. In this terrain we apply a centered source with respect to the x-direction and near from the top boundary, generating a signal which is later received by 100 geophones located at the top of the terrain and separated by 3m from each other. In order to study the behavior of the wave generated by the source, we analyze the seismic traces obtained in both boundary problems used in the homogeneous case (Fig. 6(b)).

The seismic traces corresponding to this boundary problem are show in Fig. 7. The first wave obtained between initial time and 0.05s corresponds to the direct wave generated by the source term. The primary wave corresponding to the first layer, which is located 48m deep from the source, has an arrival time of 0.077s. On the other hand, the arrival time of the secondary wave is 0.12s, which corresponds to the rebounds generated by the collision of first wave with the multiple layers. Seismic traces are in consistency with [11]. After 0.12s of simulation, seismic traces shows little reflections as a consequence of the first order absorbing boundary conditions.

With the purpose of compare the effectiveness of boundary conditions, we have considered a second problem with Dirichlet-type boundary conditions based on expressions (8), and their traces are show in Fig. 8. The simulation time in both problems is 0.15s and the time steps are close to the stability condition of the new scheme.

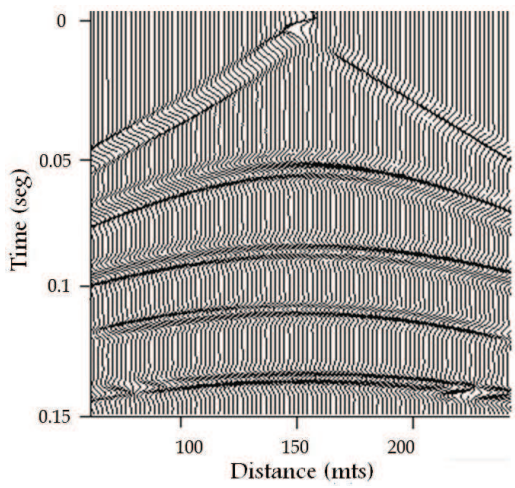

Figure 7: Seismic traces for absorbing conditions.

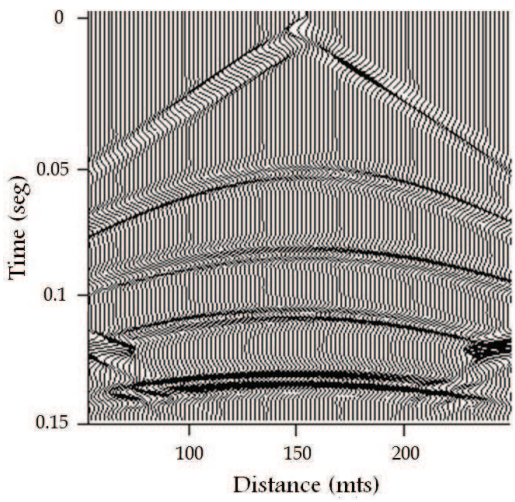

Figure 8: Seismic traces for Dirichlet conditions.

6 CONCLUSIONS

We present a new mimetic scheme based on second order finite difference for the seismic wave equation under a combination of different boundary conditions. The results that we have obtained show that the proposed scheme produce satisfactory results which are consistent with the physics of the problem, over homogeneous and heterogeneous domains

in spite of using first order boundary absorbing conditions. A convergence analysis shows that the new scheme has an stability range that enlarge that of the scheme on traditional finite difference in proportion to $\sqrt{3}$. For future works, we are planning extend to three dimensions the new scheme and to enhance the efficiency of the absorbing boundary conditions proposed by Reynolds.

REFERENCES

[1] Reynolds, A., Boundary conditions for the numerical solution of wave propagation problems. *Society of Exploration Geophysicists*, vol. 43, n. 6, pp. 1099-1110, 1978.

[2] Samarskii, A., Tishkin, V., Favorskii, A., Shashkov, M., Operational finite-difference schemes. *Differential Equations*, vol. 17, n. 7, pp. 854-862, 1981.

[3] Geoffrey, E., Day, S., Minter, J.,A support-operator method for viscoelastic wave modelling in 3-D heterogeneous media. *Geophysical Journal International*, vol. 172, n. 1, pp. 331-334, 2008.

[4] Lipnikov, K., Manzini, G., Shashkov, M., Mimetic finite difference method. *Journal of Computational Physics*, vol. 257, pp. 1163-1227, 2014.

[5] Castillo, J., Hyman, J., Shashkov, M., Steinberg, S., Fourth-and sixth-order conservative finite difference approximations of the divergence and gradient. *Applied Numerical Mathematics*, vol. 37, n. 1, pp. 171-187, 2001.

[6] Castillo, J., Grone R., A matrix analysis approach to higher-order approximations for divergence and gradients satisfying a global conservation law. *SIAM Journal on Matrix Analysis and Applications*, vol. 25, n. 1, pp. 128-142, 2003.

[7] Castillo. J, Yasuda, , M., Linear systems arising for second-order mimetic divergence and gradient discretizations. *Journal of Mathematical Modelling and Algorithms*, vol. 4, n. 1, pp. 67-82, 2005.

[8] Rojas, O., Day, S., Castillo, J. Dalguer, L., Modelling of rupture propagation using high-order mimetic finite differences. *Geophysical Journal International*, vol. 172, n. 2, pp. 631-650, 2008.

[9] Rojas, O., Dunham, E., Day, S. Dalguer, L., Castillo, J., Finite difference modelling of rupture propagation with strong velocity-weakening friction. *Geophysical Journal International*, vol. 179, n. 3, pp. 1831-1858, 2009.

[10] Rojas, O., Otero, B., Castillo, J. Day, S., Low dispersive modeling of Rayleigh waves on partly staggered grids. *Computational Geosciences*, vol. 18, n. 1, pp. 29-43, 2014.

[11] Keiswetter, D., Black, R., Schmeissner, C., A program for seismic wavefield modeling using finite-difference techniques. *Computers & Geosciences*, vol. 22, n. 3, pp. 267-286, 1996